Crack Detection in a Concrete Structure Using an Underwater Vehicle

doi: https://doi.org/10.5954/ICAROB.2021.OS23-1

Crack Detection in a Concrete Structure Using an Underwater Vehicle

Yuya Nishida[*]
Kyushu Institute of Technology
2-4 Hibikino, Wakamatsu, Kitakyushu, Fukuoka 808-0196, Japan

Naoto Sohara[*2]
Kyushu Institute of Technology
2-4 Hibikino, Wakamatsu, Kitakyushu, Fukuoka 808-0196, Japan

Shinsuke Yasukawa[*3]
Kyushu Institute of Technology
2-4 Hibikino, Wakamatsu, Kitakyushu, Fukuoka 808-0196, Japan

Kazuo Ishii[*4]
Kyushu Institute of Technology
2-4 Hibikino, Wakamatsu, Kitakyushu, Fukuoka 808-0196, Japan
*E-mail: y-nishida[*1], s-yasukawa[*3], ishii[*4]@brain.kyutech.ac.jp, sohara.naoto395@mail.kyutech.jp[*2]*
https://www.kyutech.ac.jp/

Abstract

In this paper, to realize efficient underwater infrastructure inspection, automatic crack detection by image processing is proposed. In first process of our method generates enhanced image based on the absorbance from the turbidity meter and removes background component, and then detects crack from the enhanced image by using decision tree learning algorithm. This paper explains the algorithm of our method and shows evaluation experiment results.

Keywords: Crack detection, image processing, Underwater vehicle

1. Introduction

Almost social infrastructures that were built at the time of high economic growth have become deteriorated and have a risk of accidents and traffic restrictions [1]. Japanese Ministry of Land, Infrastructure, Transport and Tourism made the road law that the infrastructures such as a bridge and tunnel should be inspected every five years, in 2014. However, infrastructure inspection is difficult with human hands alone because there are about 730,000 bridges and more than 10,000 tunnels in Japan. In particular, the inspection of underwater infrastructures is not progressing because the inspection is inefficient and dangerous to divers. Several institutes have been researched underwater infrastructure inspection method by using a ROV (Remotely Operated Vehicle) and image processing [2]. However, cracks on the underwater infrastructures are difficult to automatically detect by the image processing, because underwater images taken by the ROV depends on the water turbidity that varies from the site.

Our laboratory has been developing inspection method by using the USV (Unmanned Surface Vehicle) and ROV to realize efficiency inspection of underwater infrastructure [3]. This paper proposes crack detection method by using photo image from a camera and

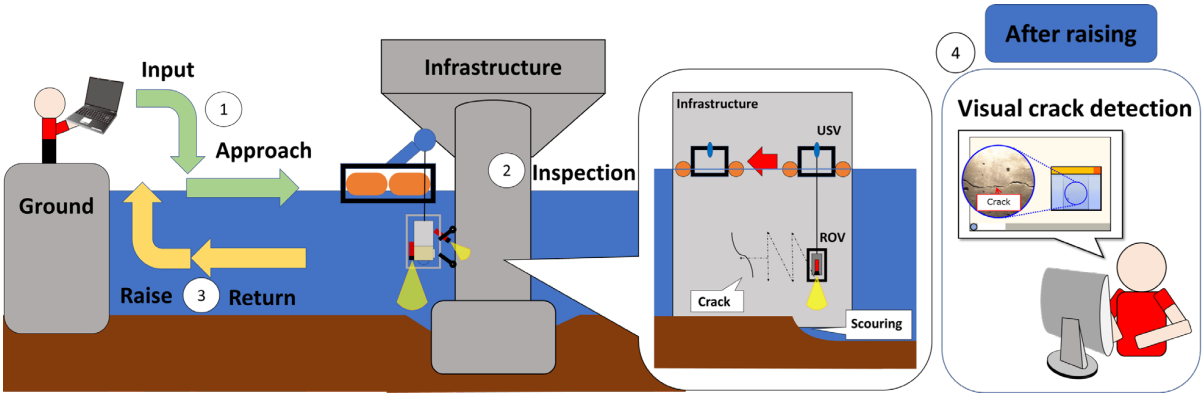

Fig. 1 Underwater infrastructure inspection by the USV and the ROV

absorbance from a turbidity meter installed on the ROV, and experiment results for the evaluation of our method are shown.

2. Underwater infrastructure inspection

2.1. *Inspection procedure*

The underwater infrastructures like valley highway pillar are located in a lake and a river that are hard for people to go. The ROV which its movement is restricted by the umbilical cable is hard to approach the infrastructures for them inspection. Our laboratory developed inspection method that a USV supports a ROV for underwater infrastructure inspection. Figure 1 shows operation overview and inspection procedure by using the USV and the ROV. The USV has four thrusters for horizontal movement, a GPS, IMU for positioning, wireless LAN for communication to the operator, and batteries. Fist, the operator deploys the USV with the ROV in the water and the USV moves to target infrastructure by heading and position controls. Second, the ROV dives by a winch mounted on the USV and captures the infrastructure images by using a front camera and a LED light. At this time, the ROV moves to horizontal direction by the USV thrusters and the ROV heading is controlled its thrusters. The ROV and the USV are connected an umbilical cable, and the operator on the quay monitors infrastructure image captured by the front camera of the ROV during inspection. After the inspection, the USV that stores the ROV returns to the quay near the operator and is recovered by the operator. Finally, cracks on the infrastructure is detected from

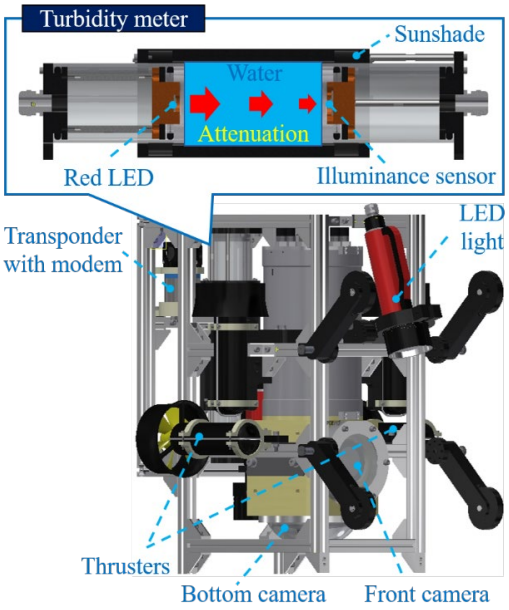

Fig. 2 The ROV equipped a turbidity meter

captured images by offline image processing that is explained in Chapter 3.

2.2. *The ROV system for inspection*

The ROV shown in Fig.2 is used for inspection of underwater infrastructure. The ROV has a front camera for crack inspection of the infrastructure and a bottom camera for scouring inspection of seafloor near the infrastructure as observation device. Two thrusters are used for that the ROV direction is controlled and the infrastructure is approached. The transponder with modem function includes the depth sensor and IMU sensor, and the USV measures the ROV position by using

it. A turbidity meter on the rear consists of a red LED, an illuminance sensor and sunshade, and surrounding water gets into the sunshade. The illuminance meter measures the red LED light intensity I' that is attenuated by the water. Relationship between Light intensity I_0 which is irradiated by the LED and I' is expressed by following the Lambert-Beer law:

$$A = -\log\left(\frac{I'}{I_0}\right) \quad (1)$$

where A denotes the absorbance that depends on the distance traveled by the light. For distance-independent values are desirable to represent the underwater light environment, equation (1) is rearranged as following.

$$\beta = -\frac{1}{d}\log\left(\frac{I'}{I_0}\right) \quad (2)$$

d denotes the distance the LED and the illuminance sensor, our turbidity meter outputs β that denotes the attenuation coefficient.

3. Crack detection method

3.1. *Preprocessing*

Cracks on the underwater infrastructure are detected by image processing from the images captured by the ROV. The image processing is separated the preprocessing and the detection process, as shown in Fig.3. The contrast between the cracks and the infrastructure surface is important for crack detection, because the cracks is detected based on the brightness, not color. First step generates high contrast images by using the absorbance coefficient from the turbidity. Second step searches crack position from the images by using the decision tree learning.

Because light in the lake and the river diffuses by floating particles such as the sand and the plankton, degraded images are taken by the ROV during the underwater infrastructure inspection. The degraded image $\boldsymbol{g}$ is represented by using raw image $\boldsymbol{f}$.

$$\boldsymbol{g} = \boldsymbol{H} * \boldsymbol{f} \quad (3)$$

where * means the convolution operation. $\boldsymbol{H}$ in equation (3) denotes point spread function and is represented multiplication of line spread functions in u and v axis of image coordinate, and those functions are approximated by the gaussian function. Undegraded image $\boldsymbol{f}$ is obtained

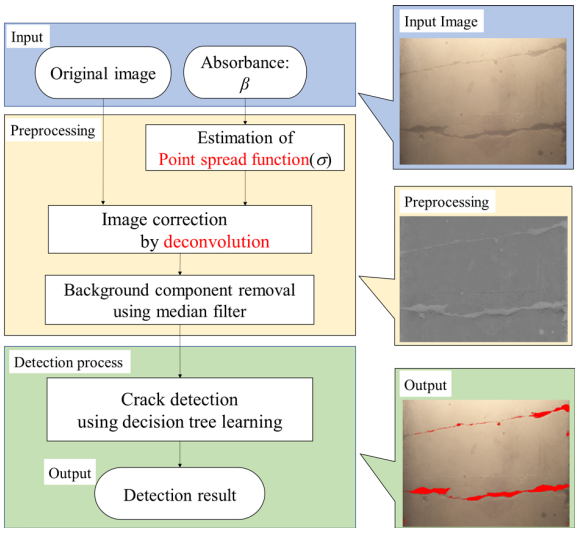

Fig. 3 Crack detection procedure

by deconvolution operation of $\boldsymbol{H}$ on equation (3). In preprocessing, this research generates high contrast image that background component is removed from $\boldsymbol{f}$ by using median filter.

3.2. *Detection process*

This process uses the decision tree learning of classification tree that can obtain complex identification boundaries by combinations of simple identification roles. The classification tree is learned by CART (classification and regression tree) that threshold for the classification is decided by following Gini coefficient [4].

$$L(t) = \sum_{j\neq 1} P(C_i|t)P(C_j|t) \quad (4)$$

$P(C_i|t)$ denotes the probability that node t in the tree selects data of class i, and $P(C_j|t)$ denotes the probability that node t in the tree selects data of class j. In the Cart, the decision tree learning is learned to maximize following equation expressed by the Gini coefficient.

$$\Delta L(t) = L(\mathrm{t}) - \{p_L L(t_L) + p_R L(t_R)\} \quad (5)$$

p_L and p_R represent the probability of being classified into left and right node. $L(t_L)$ and $L(t_R)$ denote Gini coefficients left and right nodes. In this research, the decision tree learning is learned by using equation (5) until that the node in the tree reaches 100 or more.

The input vector to the decision tree learning is 32 demission that consists of the brightness of target pixel (1), each brightness after applying 3 square median filters

(3), each brightness after applying 2 non-square median filters from 8 directions (16), each brightness after multiscale line enhancement by 11 types Hessian matrix (11) and noise candidate data (1). The brightness of target pixel is used as input vector, because the decision tree learning in this research classifies target pixel into crack and back background pixel. If only the brightness is used as input vector, false recognition can occur due to the surface color of the infrastructure. Because the brightness after applying the gaussian filters is included to input vector, classification results in the learning are less sensitive to the background color [4]. Each brightness after applying by the Hessian matrixes is used as input vector, because enhanced cracks are extracted by multi scale line enhancement using the Hessian matrixes [5]. The brightness like noise is included to the input vector, to reduce the effect of the impulse noise.

4. Experiment

4.1. *Parameter estimation*

As mentioned in chapter 3, the image taken by the ROV in the turbid water degrades based on the point spread function that is represented multiplication of the line spread functions approximated by gaussian function. However, nobody knows how the light is spread by turbid water. To analyze the relationship of the attenuation coefficient and the standard deviation for the point spread function, this research performed photographing experiment in the turbid water using the ROV with the turbidity meter. The clack scale which has lines from 0.03mm width to 1.50mm width was used for the photographing target. The turbid waters from 0 degree to 20 degrees were made by using the Kaolin which is also used for JIS turbidity standard. Figures 4 shows each picture and the brightness in the turbid waters of 0 degree and 25 degrees. At this time, target clack was 0.2mm width line that is the minimum requirement for the repair. The turbidity meter outputted 3.6 in 0 degree water and 4.64 in 25 degrees water, as attenuation coefficient. The picture in 25 degrees water was darker overall than the picture in 0 degree and the clack line were blurry. Figure 5 shows the standard deviations of approximated gaussian function in each brightness versus absorbance coefficient from the turbidity meter. This research used approximated quadratic function which fits to the

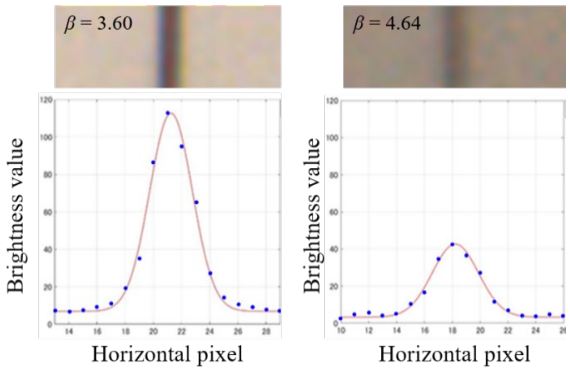

Fig. 4 Comparison of brightness distribution

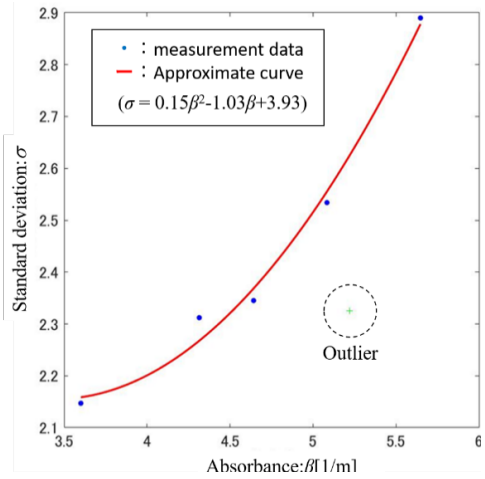

Fig.5 Absorbance coefficient vs. standard deviation

standard deviations without the one outlier data, to detect the cracks.

4.2. *Crack detection*

The cracks on the concrete block was detected by our method for evaluation. Figure 6 shows the image taken by the ROV in 25 degree water, grayscale image corrected by using the point spread function, the image with background components removed and detection results. As a result of comparing the raw image and the corrected image, the contrast of the crack edge on the corrected image was higher than the contrast of raw image cracks. Brightness unevenness and concrete pattern were removed by process using median filters. Although there were some cracks that could not be detected, our method detected the cracks with few false positives. Table 1 shows accuracy rage and sensitivity with and without the correction by the point spread

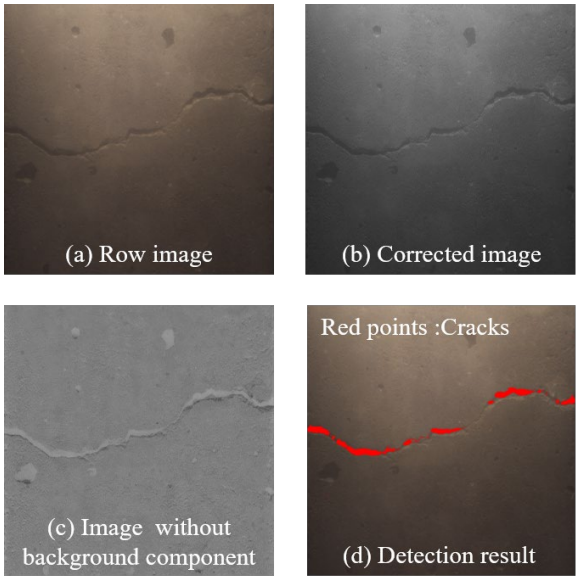

Fig.5 Absorbance coefficient vs. standard deviation

function. Although performance of the crack detection with and without the correction was almost same until 10 degrees water, the accuracy rate and the sensitive were improved with turbidity from 15 degrees to 20 degrees, and the sensitivity of our method was greatly increased. This means that the detection rate was improved by the correction using the point spread function.

5. Conclusions

This paper explains efficient underwater structure inspection by using the USV and the ROV, and the crack detection method in the turbid water is proposed. The underwater infrastructure is observed by the ROV equipped the turbidity meter which can measure the absorbance coefficient of the turbid water. In preprocess, the image taken by the ROV is corrected by using the point spread function and high contrast image is generated by using median filters. Our method detected cracks on the underwater infrastructure in the turbid water from the image enhanced by the preprocess, with high accuracy rate.

Table 1 Accuracy rate and sensitive in each turbidity

Turbidity	Accuracy rate		Sensitivity	
	With correction	No correction	With correction	No correction
0	0.992	0.990	0.583	0.358
5	0.996	0.995	0.729	0.713
10	0.995	0.995	0.655	0.672
15	0994	0.990	0.625	0.586
20	0.994	0.974	0.642	0.425
25	0.994	0.972	0.5851	0.294

References

1. Road Bureau, Aging of social infrastructure, Current statu s of aging and issues related to aging countermeasures, Ja panese Ministry of Land, Infrastructure, Transport and To urism, https://www.mlit.go.jp/hakusyo/mlit/h25/hakusho/h26/html/n1131000.html, *in Japanese*
2. Sugimoto Hideki, et al., Underwater Structure Diagnosis System by Remotely Operated Vehicle, Journal of the Robotics Society of Japan, Vol.34, No.8, pp.505-506, 2016, *in Japanese*
3. Takumi Ueda, et al., Inspection system for underwater structure of bridge pier, Proc. of International Conference on Artificial Life and Robotics, DOI: 10.5954/ICAROB.2019.OS21-2, Beppu, 2019
4. Naoya Kuramoto, et al., Detection of pavement crack from image by decision tree learning, Journal of Japan Society of Civil Engineers, Vol.71, No.2, pp.823-830, 2015, *in Japanese*
5. Yusuke Fujita, et al., Automatic and exact crack extraction from concrete surfaces using image processing techniques, Doboku Gakkai Ronbunshuu F, Vol.66, No.3, pp.459-470, 2010, *in Japanese*